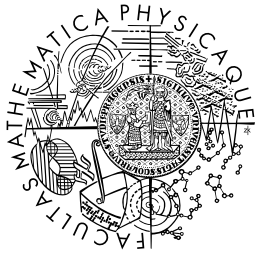

FACULTY
OF MATHEMATICS
AND PHYSICS
Charles University

Summary of doctoral thesis

Hana Jakoubková

Earthquake swarms in diverse tectonic environments: West Bohemia and Southwest Iceland

Department of Geophysics

Supervisor of the doctoral thesis: Ing. Josef Horálek, Csc.
Study programme: Physics
Study branch: Geophysics

Prague 2018

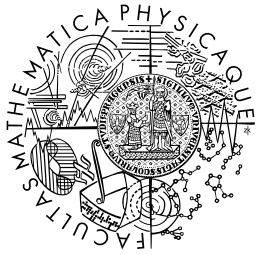

MATEMATICKO-FYZIKÁLNÍ FAKULTA
Univerzita Karlova

Autoreferát dizertační práce

Hana Jakoubková

Zemětřesné roje v různých tektonických prostředích: západní Čechy a jihozápadní Island

Katedra Geofyziky

Vedoucí dizertační práce:	Ing. Josef Horálek, Csc.
Studijní program:	Fyzika
Studijní obor:	Geofyzika

Praha 2018

Dizertace byla vypracována na základě výsledků získaných v letech 2008-2017 během doktorandského studia na Katedře geofyziky MFF UK. Použitá data byla pořízena za podpory Geofyzikálního ústavu AV ČR, v.v.i.

Dizertant:
Mgr. Hana Jakoubková
Geofyzikální ústav AV ČR, v.v.i.
Boční II/1401, 141 31 Praha 4

Školitel:
Ing. Josef Horálek, Csc.
Geofyzikální ústav AV ČR, v.v.i.
Boční II/1401, 141 31 Praha 4

Oponenti:
RNDr. Jiří Málek, Ph.D.
Ústav struktury a mechaniky hornin AV ČR, v.v.i.
V Holešovičkách 41, 182 09 Praha 8

Dr. Simone Cesca
Helmholtz-Zentrum Potsdam
Deutsches GeoForschungsZentrum GFZ
Telegrafenberg, 14473 Potsdam

Předseda oborové rady:
Prof. RNDr. Jiří Zahradník, DrSc.
Katedra geofyziky MFF UK
V Holešovičkách 2, 180 00 Praha 8

Autoreferát byl rozeslán dne

Obhajoba dizertace se koná dne 25. 9. 2018 v 10:00 hodin před komisí pro obhajoby dizertačních prací v oboru Geofyzika v budově Geofyzikálního ústavu AV ČR, v.v.i., Boční II/1401, 141 31 Praha 4, v zasedací místnosti ústavu.

S dizertací je možno se seznámit v PGS MFF UK, Ke Karlovu 3, Praha 2

Contents

Introduction

A seismic activity can be generally classified either as a common earthquake, called mainshock-aftershock sequence, or an earthquake swarm. The mainshock-aftershock sequence is characterised by a dominant earthquake (mainshock) followed by a series of aftershocks with magnitudes usually by one or more magnitude units lower than that of the mainshock (Fig. 1a). An earthquake swarm is a series of earthquakes closely clustered in space and time, without a dominant event (Mogi, 1963) (Fig. 1b).

Earthquake swarms occur worldwide both on the boundary of tectonic plates (interplate swarms) and inside plates (intraplate swarms). In my doctoral thesis I analyse earthquake swarms from two completely different tectonic areas:

West Bohemia/Vogtland (interplate) and Southwest Iceland (intraplate), from the perspective of statistical characteristics (magnitude-frequency distribution, interevent time distribution), seismic moment release and space-time distribution of events with the aim of finding the swarm characteristics which are dependent/independent on the tectonic environment and which differentiate earthquake swarms from mainshock-aftershock sequences. Namely I analysed the intraplate earthquake swarms from West Bohemia in 1997, 2000, 2008, 2011, 2017 together with the non-swarm activity in 2014, and the Icelandic interplate swarms from the Krísuvík geothermal field (Reykjanes Peninsula) in 2003 and 2017, the Hengill volcanic complex in 1997, and the Ölfus area (the edge of the South Iceland Seismic Zone where typically mainshock-aftershock earthquakes occur) in 1998. In addition, I derived 3D structure of the main focal zone Nový Kostel and retrieved prevailing focal mechanisms in the 2011 swarm and in the 2014 non-swarm sequence.

Prior to analyses I improved the estimation of local magnitude M_L by the West Bohemian network WEBNET, and adapted the formula for computing M_L by the regional network SIL for the M_L estimation by local network REYKJANET in Iceland. Besides, I derived the scaling relation between local magnitude M_L by WEBNET and seismic moment M_0, and performed synthetic tests to evaluate location errors yielded by the hypoDD code when applied to the WEBNET data.

Most of the results regarding the West Bohemia earthquake activities, which are presented in this thesis, have been published in the papers by Čermáková and Horálek (2015) and Jakoubková et al. (2017), the results concerning Southwest Icelandic swarms have not been published yet.

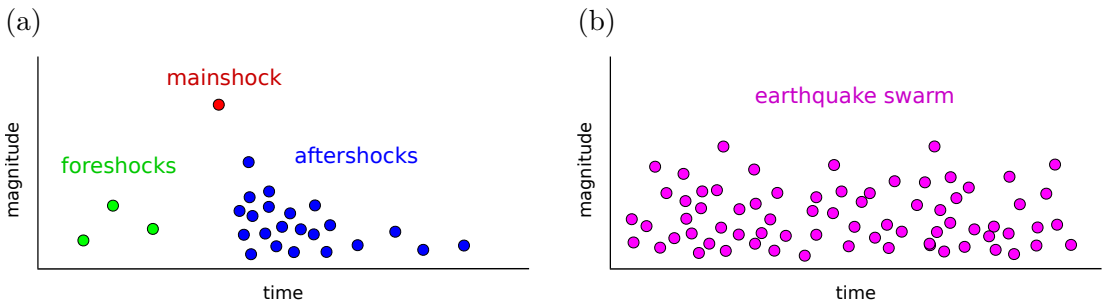

Figure 1: Schematic magnitude-time distribution of events in case of mainshock-aftershock sequence (a) and earthquake swarm (b). In (a), *red dot* - mainshock, *green dots* - foreshocks, *blue dots* - aftershocks. *Violet dots* in (b) - swarm-like events.

1. The areas of interest

1.1 West Bohemia/Vogtland region

West Bohemia/Vogtland (latitude $\approx 49.8-50.7$°N, longitude $\approx 12-13$°E) is well known for recurring of intraplate earthquake swarms and enormous emanations of CO_2, which are usually attributed to Quaternary volcanism. The region is located in the western part of the Bohemian Massif, where three tectonic units: the Saxothuringian, the Teplá-Barrandian and the Moldanubian, merge (e.g., Babuška et al., 2007). The region is intersected by the NE-SW trending Eger rift and NNW-SSE striking Mariánské Lázně fault (ML fault, see Fig. 1.1).

Seismicity in the region is permanent, mainly of the swarm-like character, the strongest events are mostly with magnitudes $M_L < 4.0$; the most intense earthquake activities in the last hundred years were the M_L4.6 earthquake swarm in 1985/86 and the M_L 4.4 mainshock-aftershock sequence in 2014. Since 1991, seismicity in the region has been monitored by a local seismic network WEBNET consisting of 23 stations at present. Distribution of of the $M_L \geq 0$ events from the period of 1997 – 2015 together with the WEBNET stations are depicted in Fig. 1.1.

All larger swarms ($\sim M_L > 2.5$) are located in the focal zone Nový Kostel (NK) which dominates the seismicity of the whole region (e.g., Fischer et al., 2014). Notable swarms occurred there in 1997 (M_L3.0), 2000 (M_L3.3), 2008 (M_L3.8), 2011 (M_L3.7), 2013 (M_L2.3) and 2017 (M_L3.1), an exceptional non-swarm activity comprising three mainshock-aftershock sequences (M_L 3.5, 4.4 and 3.6) occurred in 2014. Brief characteristics of significant seismic activities that have occurred in the NK zone since 1991 and that I analyse in my thesis are given in Tab. 1.1.

Activity	Duration [days]	Num. of ev. ($M_L \geq 0$)	M_{Lmax}	Character
1997	14	500	3.0	swarm
2000	71	3840	3.3	swarm
2008	28	4400	3.8	swarm
2011	12	5740	3.7	swarm
2013	33	270	2.3	mini-swarm
2014	12	2800	4.4	M-A sequence
2017	16	2500	3.1	swarm

Table 1.1: Basic characteristics of the West Bohemian activities. Duration of each activity indicates number of days during which 90% of events, which were recorded within three months, occurred.

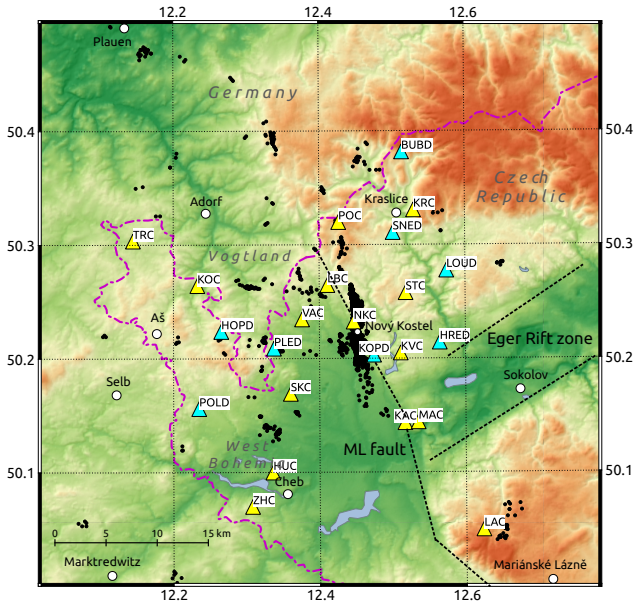

Figure 1.1: Map of the seismically active area in the West Bohemia/Vogtland region with stations of the WEBNET network. *Yellow and light blue triangles* - WEBNET stations. *Black dots* - seismic events of $M_L \geq 0$ from the time period 1997-2017. *Larger white circles* - towns, *smaller white circle* - village of Nový Kostel. *Dashed lines* mark dominant tectonic structures in the region: the Mariánské-Lázně fault (ML) and the Eger Rift zone. *Dot-dashed violet line* denotes the Czech-German border.

1.2 Iceland - brief characteristics

Iceland is a volcanic island in the North Atlantic Ocean spanning a divergent Mid-Atlantic Ridge boundary between the Eurasian and North American tectonic plates. Iceland lies above a hotspot, the Iceland plume, which is partly responsible for the high volcanic activity and also has formed Iceland itself (Allen et al., 1999, 2002b,a). The interaction between the Iceland plume and the Mid-Atlantic Ridge has formed complex rifting zones and a series of volcanic and seismic transform zones (Fig. 1.2) (Einarsson, 2008).

Seismicity in Iceland is persistent. Ordinary earthquakes of the mainshock-aftershock type typically occur in the shear zones South Iceland Seismic Zone (SISZ) and Tjörnes Fracture Zone (TFZ). Earthquake swarms are characteristic of the Reykjanes Peninsula (RP), Hengill triple-junction area, and offshore areas of Iceland. Seismicity on the whole Icelandic territory has been monitored by a regional network SIL since 1990, currently, the SIL consists of 68 stations that are spread all over Iceland.

In my thesis I focus on the Reykjanes Peninsula and adjacent Hengill volcanic complex which stretch along the Reykjanes Ridge; it represents a belt roughly 80×25 km (latitude $\approx 63.8 - 64.05$°N, longitude $\approx 21.45 - 22.75$°W). On the RP the plate boundary forms a pronounced oblique rift along the whole peninsula in length of about 65 km, the plate motion rate is about 20 mm/year in E-W direction and about 5 mm/year perpendicular to it (Geirsson et al., 2010); thus the RP exhibits the highest geodynamic activity in Iceland (Sæmundsson and Einarsson, 2014).

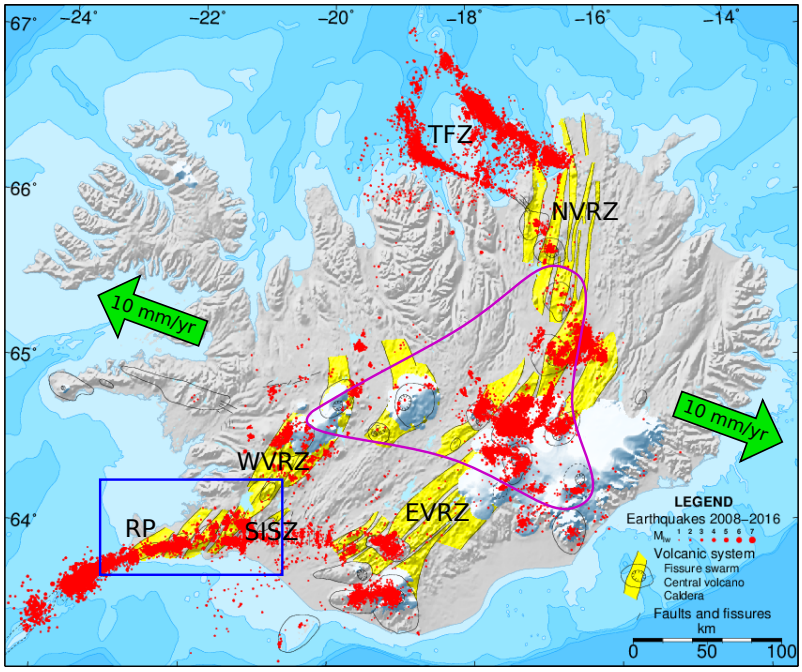

Figure 1.2: Distribution of seismic events in Iceland in the period 2008 – 2016 (*red dots*). The region of my interest is indicated by *blue rectangle*. RP - Reykjanes Peninsula, SISZ - South Iceland Seismic Zone, WVRZ - Western Volcanic Rift Zone, EVRZ - Eastern Volcanic Rift Zone, NVRZ - Northern Volcanic Rift Zone, TFZ - Tjörnes Fracture Zone. The *green arrows* indicate the plate motion. *Violet counter* - Iceland plume at 350 km depth.

The peninsula is one of the most seismically active parts of Iceland, especially at the microearthquake level ($M_L < 3$). Since 2013, swarm-like seismicity on the Reykjanes Peninsula has been monitored by the REYKJANET network, operated by the Institute of Geophysics and Institute of Rock Structure and Mechanics of the Czech Academy of Sciences. REYKJANET comprises 15 autonomous broadband stations covering the area roughly 60×20 km.

The Hengill region is a highly complex portion of the plate boundary, located at the intersection of three tectonic systems: the Reykjanes Peninsula, the Western Volcanic Zone, and the South Icelandic Seismic Zone (transform shear zone). The complexity of the region contributes substantially to the seismic activity. The Ölfus region is a transition area between the Hengill triple junction and

Activity	Duration [days]	Num. of ev. ($M_L \geq 0$)	M_{Lmax}	M_{Lw}
Hen 1997	54	4850	4.4	4.7
Ölf 1998	28	5130	4.9	5.1
Krí 2003	6	1160	4.3	5.0
Krí 2017	6	1660	3.9	4.1

Table 1.2: Basic characteristics of the swarms in Southwest Iceland. Hen - Hengill, Ölf - Ölfus, Krí - Krísuvík. Duration of each activity indicates number of days during which 90% of events, which were recorded within three months, occurred.

SISZ situated about 15 km to the south from the Hengill central volcano. Both earthquake swarms and normal earthquakes (mainshock-aftershock sequences) occurred there (Jakobsdóttir, 2008).

In my thesis I investigated two individual earthquake swarms from the Hengill-Ölfus activity in 1997/98, and two short swarms from the Reykjanes Peninsula (Krísuvík area) in 2003 and 2017. Brief characteristics of the analysed Icelandic swarms are shown in Tab. 1.2, their mutual position in Fig. 1.3.

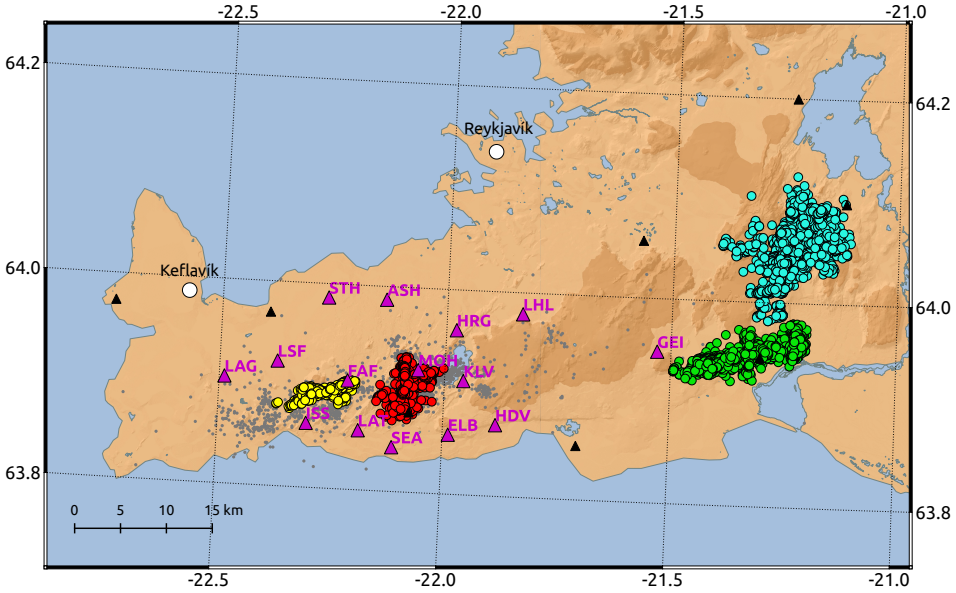

Figure 1.3: Map of Southwest Iceland with locations of the four earthquake swarms of my interest: the swarm of Hengill in 1997 (*light blue circles*), in Ölfus in 1998 (*green circles*), and the two swarms in the Krísuvík area in 2003 (*red circles*) and 2017 (*yellow circles*). The *gray dots* - seismicity in period 2013–2017 recorded by the REYKJANET stations. *Violet triangles* - stations of the REYKJANET network, the smaller *black triangles* - stations of the SIL network.

2. Data and velocity models

West Bohemia/Vogtland data used are solely from WEBNET. Southwest Iceland data which I used are of two types: (1) The catalogue data of Icelandic network SIL from the time period 1991 – 2009 provided by the Icelandic Meteorological Office, and (2) data of local seismicity on the Reykjanes Peninsula in 2013 – 2017 from our network REYKJANET.

As regards the West Bohemia earthquake-swarm region, I used the 1-D vertically inhomogeneous isotropic velocity model of the upper crust published by Málek et al. (2005). As for Southwest Iceland, the 1-D vertically inhomogeneous isotropic velocity model by Stefánsson et al. (1993) (SIL velocity model) was used.

3. Investigations prior to analysis

3.1 WEBNET and REYKJANET magnitudes and their calibration

The WEBNET local magnitude M_L has been calculated by formula by Horálek et al. (2000) introduced in 1993; that time the WEBNET network comprised five stations only. Because the number of online stations of WEBNET increased step by step up to existing 15 ones (Fig. 1.1), I upgraded the M_L estimation by WEBNET. I recalculated station corrections C_i for all the available stations (Tab. 3.1) and the constants in the formula (3.1), for this purpose I applied the classical iterative approach. The new formula for the local WEBNET magnitude is as follows:

$$M_{Li} = \log A_{Smax} - \log 2\pi + 2.1 \cdot \log R_i + C_i - 1.2, \tag{3.1}$$

where M_{Li} is the magnitude of the i-th station, A_{Smax} is the absolute value of the maximum total amplitude of the S-wave ground velocity measured in µm/s, 2.1 is a constant involving intrinsic attenuation and scattering of the S-wave, R_i is the hypocentral distance of the station in km, C_i is the station correction, and -1.2 is a calibration constant. A final local magnitude M_L of an event is calculated as the average of the station magnitudes M_{Li}. The problems of improving the WEBNET local magnitudes and results obtained have been published in Čermáková and Horálek (2015).

	KAC	KOC	KRC	KVC	LAC	LBC	NKC
C_i	-0.393	-0.013	-0.128	0.103	-0.132	0.133	0.093
	POC	SKC	STC	TRC	VAC	ZHC	
C_i	0.038	0.081	0.107	0.135	0.017	-0.240	

Table 3.1: Station corrections for 13 permanent WEBNET stations.

Magnitudes of Icelandic earthquakes recorded by the network SIL are provided by the Icelandic Meteorological Offce (IMO) that is responsible for monitoring of seismicity in Iceland. Two types of magnitudes in the SIL network are used: a local magnitude M_L and a local moment magnitude, denoted M_{Lw} or $M_L(M_0)$. The SIL local magnitude has been calculated by the formula (Jakobsdóttir, 2008):

$$M_L = \log A_{Smax} + 2.1 \cdot \log D - 4.8, \tag{3.2}$$

where A_{Smax} is the maximum of the ground velocity amplitude (filtered by a high-pass filter with the corner frequency of 2 Hz) in an interval of 10 seconds around the S-wave which is measured in nm/s, D is a hypocenter distance of the station in km, and -4.8 is a calibration constant (Jakobsdóttir, 2008). Interestingly, the formula (3.2) is very similar to the formula (3.1) for M_L by WEBNET, although the two formulas were derived fully independently.

In the SIL catalogues the local magnitude M_L is mostly used. However, the SIL local magnitude scale saturates around $M_L 5.5$ (due to HP filter of 2 Hz), so the largest events are reported only with local moment magnitude M_{Lw} (Dr. Gunnar B. Guðmundsson, IMO, personal communication).

As regards the magnitude estimation from the REYKJANET network we benefit from similarity of the formulas for M_L by WEBNET (3.1) and by SIL (3.2) which allows us to determine M_L of events recorded by REYKJANET using our formula (3.1). For this purpose I calculated corrections C_i for all 15 REYKJANET stations (Tab. 3.2), by the same iterative approach as in case of C_i for WEBNET. The formula used for the REYKJANET local magnitude determination is:

$$M_{Li} = \log A_{Smax} - \log 2\pi + 2.1 \cdot \log R_i + C_i - 1, \tag{3.3}$$

where C_i are corrections of the REYKJANET stations.

	ASH	ELB	FAF	GEI	HDV	HRG	ISS	KLV
C_i	0.561	0.102	-0.382	0.005	-0.528	0.158	0.104	-0.182
	LAG	LAT	LHL	LSF	MOH	SEA	STH	
C_i	0.395	-0.062	0.144	-0.146	-0.241	-0.021	0.069	

Table 3.2: Station corrections for 15 REYKJANET stations.

3.2 Scaling relation between local magnitude and seismic moment

Seismic moment M_0 is an important physical measure of the size of an earthquake defined as $M_0 = \mu AD$ (where μ is the shear modulus, A is the area of the rupture, and D is displacement along the fault after the rupture) but its determination directly from seismograms is not possible. There are three completely different empirical scaling relations between local magnitude M_L and seismic moment M_0 for the West Bohemia: by Hainzl and Fischer (2002), Michálek and Fischer (2013)

and Horálek and Šílený (2013), see Fig. 3.1. Therefore, I revised the M_L–M_0 scaling relation by means of independent data and method. I selected and processed fifteen M_L 2.0 – 4.4 events from the 2014 sequence for which Vavryčuk calculated scalar seismic moments (personal communication). Linear regression of the $\log_{10} M_0$ vs. M_L data yields the $M_L - M_0$ scaling relation

$$\log_{10} M_0 = 1.10 \cdot M_L + 10.09, \tag{3.4}$$

where M_0 is measured in Nm. An important finding is that the seismic moments by Vavryčuk are quite close to those estimated using the Horálek and Šílený (2013) relation which was derived on a rather narrow range of M_L 1.7 – 3.1 of the 2000-swarm events.

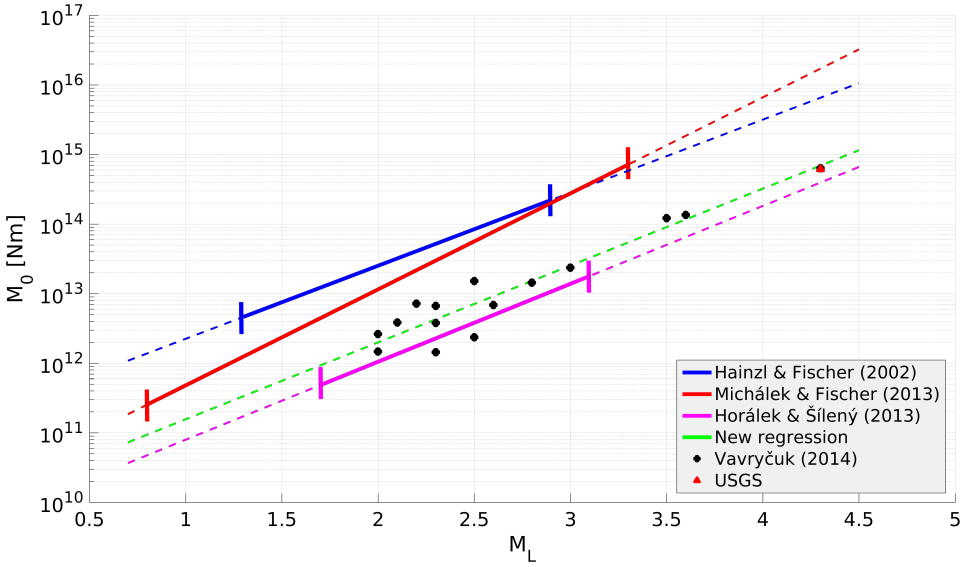

Figure 3.1: Scalar seismic moment M_0 versus the WEBNET local magnitude M_L for the scaling relation based on the 2014 events (*dashed green line*), and for the prior relations by Horálek and Šílený (2013) (*violet line*), Michálek and Fischer (2013) (*red line*), and Hainzl and Fischer (2002) (*blue line*). *Black dots*: M_0-M_L relation of 2014 events used for the M_0–M_L linear regression. *Red triangle*: $M_0 = 6.16 \times 10^{14}$ Nm ($\sim M_w = 3.8$) reported by USGS for the M_L4.4 mainshock. *Solid parts* of the blue, red and violet lines indicate the magnitude range of the events used to derive the corresponding relations.

All the seismic moment studies related to the West Bohemia activities, which are given in my thesis, are based on formula (3.4). The issue of the scaling relation between M_L by WEBNET and M_0 has been published in Jakoubková et al. (2017).

As regards the seismic moment estimation of events form Southwest Iceland I used the local moment magnitude M_{Lw} provided by IMO that is related with seismic moment M_0 according to formula

$$M_{Lw} = \log_{10} M_0 - 10, \qquad (M_{Lw} \leq 2.0) \tag{3.5}$$

and its modifications for higher magnitudes M_{Lw} (Dr. Gunnar B. Guðmundsson, IMO, personal communication).

3.3 Locating earthquakes

An exact location of an earthquake source is one of the most important tasks in my thesis. All the events used have been located in two steps: (1) absolute locating of each single event by program NonLinLoc (NLLoc; Lomax et al., 2000, 2009) and (2) refined relative localization applying the "Double difference localization" algorithm (hypoDD; Waldhauser and Ellsworth, 2000; Waldhauser, 2001) to the absolute hypocenter locations (obtained by NLLoc). This way I relocated all the West Bohemia events since 1991 using a set of stations as much consistent as possible throughout the whole analysed time period. The P- and S-wave travel time differences in event pairs in the hypoDD code can be obtained either from catalogue data or from cross-correlation of the two event waveforms. Since I worked with manually picked arrival times which were sufficiently precise, I used only catalogue data to get the travel time differences.

In the hypoDD code several input parameters are used to constrain properly neighbours of each event for which the travel time differences are calculated. Optimum parameters depend on the size of a particular focal cloud, on the number and density of events, and on the distribution of stations. I performed a number of tests to optimize these parameters to be identical for most of West Bohemia/Vogtland and Southwest Iceland activities.

I also tested the accuracy of the West Bohemia/Vogtland event locations when the hypoDD code is applied to the WEBNET data. I created six clusters of synthetic West Bohemia events varying in the number of events, shape, depth, and position relative to the WEBNET stations and relocated them with randomly perturbed data and various configurations of the stations. The tests showed well-preserved shape of all the event clusters situated within the network and slightly deformed shape of the clusters situated at the edge or outside the network. The location errors were a few tens meters for the horizontal components and slightly higher at depth (lower than 50 m). Very low location errors were found even if only four suitably distributed stations along the edge of the network were used.

4. Analysis

4.1 Statistical characteristics

4.1.1 Magnitude-frequency distribution

A magnitude-frequency distribution (MFD) of both aftershock sequences and earthquake swarms typically follow the Gutenberg-Richter law (GR law):

$$\log N = a - bM, \tag{4.1}$$

where N is a number of events having a magnitude $\geq M$. The b-value signifies the ratio of small to large events, the constant a is the event productivity of a seismic sequence, i.e. number of the $M_L \geq 0$ events in the individual activities. It is generally thought that b-values of common mainshock-aftershock sequences are ≈ 1.0 or lower, while earthquake swarms typically exceed 1.0 and are often as high as 2.5 (e.g., Lay and Wallace, 1995), which implies prevalence of small events against larger ones in individual swarm activities. The Gutenberg-Richter law is a very useful tool of earthquake statistics but without any physical meaning due to the magnitude scale dependence of the constants a and b. However, thanks to similarity of the formulas (3.1) and (3.2) for estimation of local magnitudes by WEBNET and by SIL we are able to compare MFDs of West Bohemian and Southwest Icelandic activities.

To compute a correct MFD, a complete catalogue of events with magnitudes $M_L \geq M_C$ (where M_C is a magnitude of completeness), is necessary. It is apparent that completeness magnitudes differ for individual activities. In order to get comparable results I set M_C for all the analysed activities to be $M_C = 0.25$ except for the Krísuvík swarms in 2003 and 2017, for which the higher values, $M_C = 0.50$ and 0.30 are set.

The MFDs for the activities investigated are depicted in Fig. 4.1a. Even though the West Bohemia/Vogtland and Southwest Iceland are of an entirely different tectonic character, most of events of each activity obey the GR law with the b-value 1.0 regardless of whether they are an earthquake swarm or a mainshock-aftershock sequence. However, the events at the highest magnitude level are apparently deflected from the linear trend of the GR curve downwards, besides the MFDs show pronounced magnitude gaps between the strongest events and the following weaker events. In these aspects, the MFD of all the West Bohemia and Southwest Iceland swarms point to the characteristics of the mainshock-aftershock sequences. A typical mainshock-aftershock character of the MFD is nicely seen in case of the 2014 West Bohemian activity where the three mainshocks are clearly away from the GR curve. So I infer that the swarms may be comprised of overlapping aftershock sequences, each of them dominated by a "mainshock".

Constant a (event productivity) provides a relevant estimate of the $M_L \geq 0$ events in the individual activities. The MFDs of the West Bohemia swarms show the event productivity a increase with increasing M_{Lmax} (the higher M_{Lmax} the higher a for similar b-values, b $\approx$ 1 in our case). But it does not apply in case of the M_L4.4 non-swarm activity in 2014, for which a is much smaller. The reason is that the greater part of the 2014 total seismic moment released in the

three mainshocks (M_L3.5, 4.4 and 3.6). It suggests that mainshock-aftershock sequences generally comprise much fewer events than earthquake swarms to release similar seismic moment. The MFDs of the Southwest Icelandic activities point to strikingly small event productivity of the two earthquake swarms in the Krísuvík region when compared to the Hengill volcanic complex, as well as to all the West Bohemian swarms with $M_{Lmax} \geq$ 3.3. It indicates that the swarms in the Krísuvík geothermal area may be of different character than the Hengill and West Bohemian swarms.

(a)

(b)

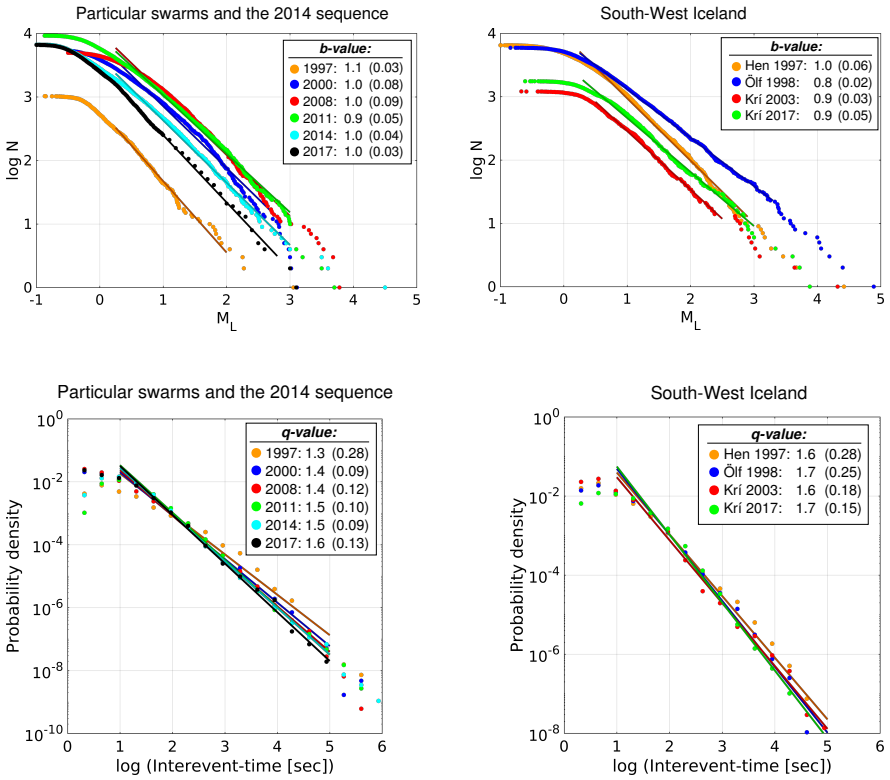

Figure 4.1: (a) Cumulative magnitude-frequency distribution (MFD), (b) probability density function of interevent times. For both (a) and (b): *Left* - the West Bohemian swarms of 1997 *(orange)*, 2000 *(blue)*, 2008 *(red)*, 2011 *(green)*, 2017 *(black)* and the non-swarm activity 2014 *(light blue)*; *Right* - the Southwest Icelandic swarms of Hengill *(orange)*, Ölfus *(blue)*, Krísuvík 2003 *(red)* and Krísuvík 2017 *(green)*. The numbers in brackets represent RMS of the linear regression.

4.1.2 Interevent time distribution

In order to evaluate the event rate of the West Bohemian and Southwest Icelandic earthquake swarms I analysed the distribution of interevent times T_w (i.e. delay times between two successive events) of all the earthquake activities concerned. For each activity I computed the T_w probability density function (PDF) for the $M_L \geq M_C$ events, the results are presented in the Fig. 4.1b. I found that the PDFs of all the West Bohemian swarms, the 2014 non-swarm sequence, and all the Southwest Icelandic swarms complied nicely with the power law T_w^{-q} (and consequently with the modified Omori law $N = k(T_w)^{-q}$, where N is a number

of interevent times T_w, and k is fault-dependent constant), which indicates that all these activities are of the Omori-like mainshock-aftershock type.

The q-values vary between 1.3 and 1.6 for the West Bohemian activities and 1.6 and 1.7 for the Southwest Icelandic ones, which implies comparable event rate (rapidity) of all these activities, nevertheless the rapidity of the Icelandic swarms is evidently higher.

It is also worth mentioning that the PDFs of the aftershocks of the individual 2014 mainshock-aftershock sequences strikingly differ, indicating the q-value 1.4 for the $M_L3.5$ (May 24), 1.8 for the $M_L4.4$ (May 31), and 1.2 for the $M_L3.6$ (August 3) episodes. It implies that rapidity (event rate) of the aftershocks of the $M_L4.4$ sequence was much higher than that of both the $M_L3.5$ and $M_L3.6$ aftershocks, and all the swarms in West Bohemia and Southwest Iceland.

4.2 Temporal development of the activities and the seismic moment release

I analysed the time course of the activities and seismic moment release, and its rate for the individual activities to get deeper insight into their nature. The time courses of the activities are represented by magnitude-time plots in Fig. 4.2. The total seismic moments M_{0tot} and local magnitudes M_{Ltot} or M_{Lw} of corresponding hypothetic single events for the individual West Bohemian and Southwest Icelandic activities are given in Tables 4.1 and 4.2, respectively. I analysed the time course of the seismic moment release (Fig. 4.3a) and the rate of the seismic moment release (Fig. 4.3b). For the latter I calculated the normalised cumulative seismic moment by the following way: The cumulative seismic moment per day is divided by the total seismic moment, these daily values are sorted in descending order, and then their cumulative distribution is computed. As a criterion for estimation of the rate of the seismic moment release I used the period during which 95% of total seismic moment was released.

The patterns of the temporal event distribution and of the seismic moment release in the individual activities are given in Figs. 4.2 and 4.3. The activities evidently differ (e.g., in duration and number of phases, number of dominant events and their magnitudes M_L, or in total seismic moment M_{0tot}), nevertheless, the patterns show some characteristic features of the West Bohemian or Southwest Icelandic activities:

- Normalised cumulative seismic moments of the activities from both regions (Fig. 4.3b) indicate generally higher rate of the seismic moment release in the Southwest Icelandic swarms compared to that in the West Bohemia swarms.

- The step-by-step seismic moment release is typical for the West Bohemia swarms. On the contrary, the Southwest Icelandic swarms are characterised by one dominant phase during which the most of seismic moment released (Fig. 4.3a), so these swarms resemble mainshock-aftershock sequences, e.g., the West Bohemian $M_L4.4$ mainshock-aftershock sequence in 2014.

- As for the West Bohemian activities, the total seismic moment released, M_{0tot}, accelerated in each subsequent activity starting from the 2000 swarm

up to the 2014 sequence and 2017 swarm (Figs. 4.2 and 4.3). It indicates that the increasing rate of the seismic moment release could be connected with a transition from the swarm-like to the mainshock-aftershock character of the 2014 and possibly of the 2017 seismicity.

- Although the 2008, 2011 and 2014 West Bohemia activities show similar size of M_{0tot}, the time course of the seismic moment release is fairly different which implies different number and magnitudes of strong events, and consequently different maximum ground motions in each activity. It is obvious that an earthquake swarm produces number of strong events to release the same seismic moment as a mainshock.

(a)

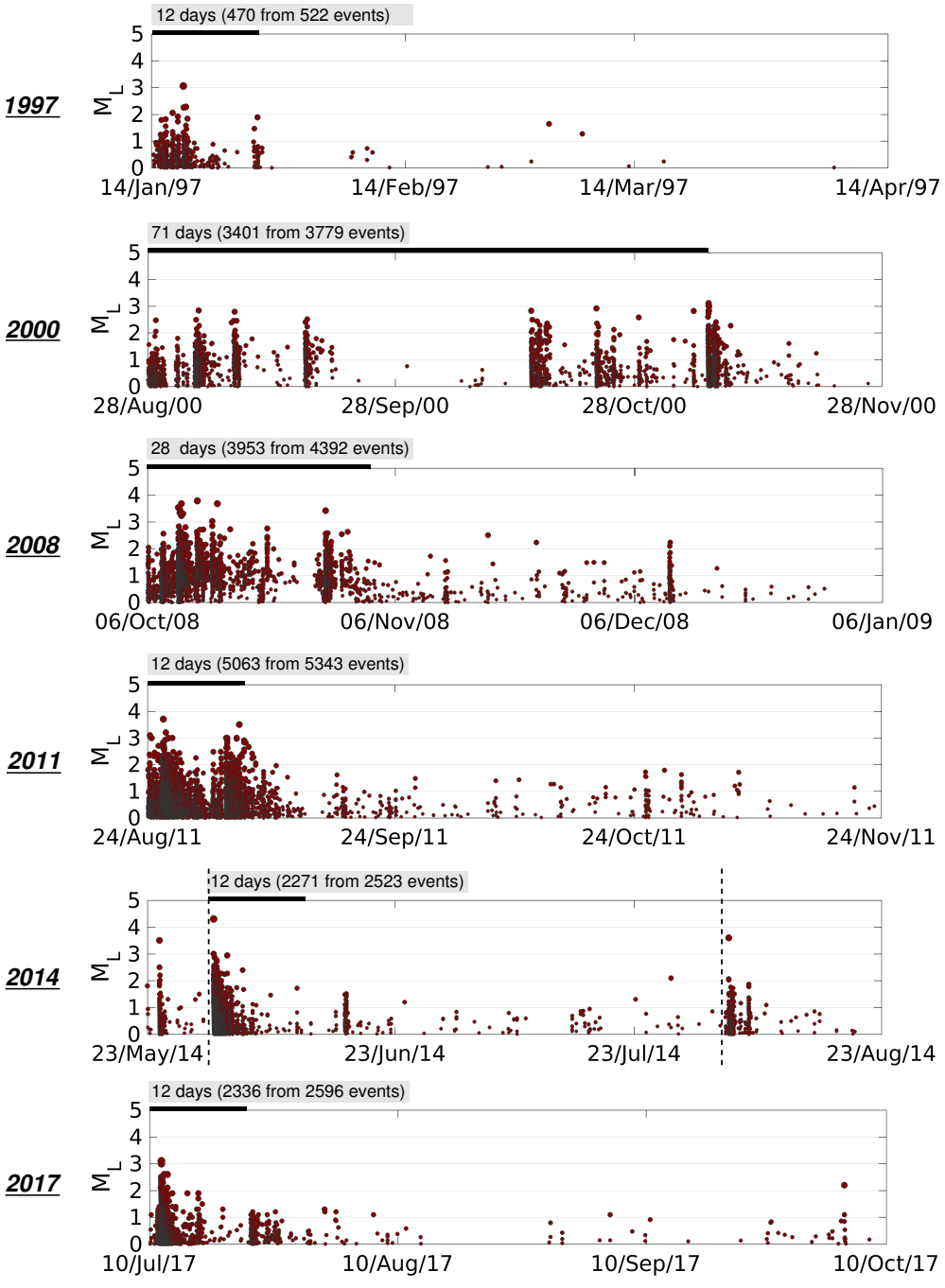

(b)

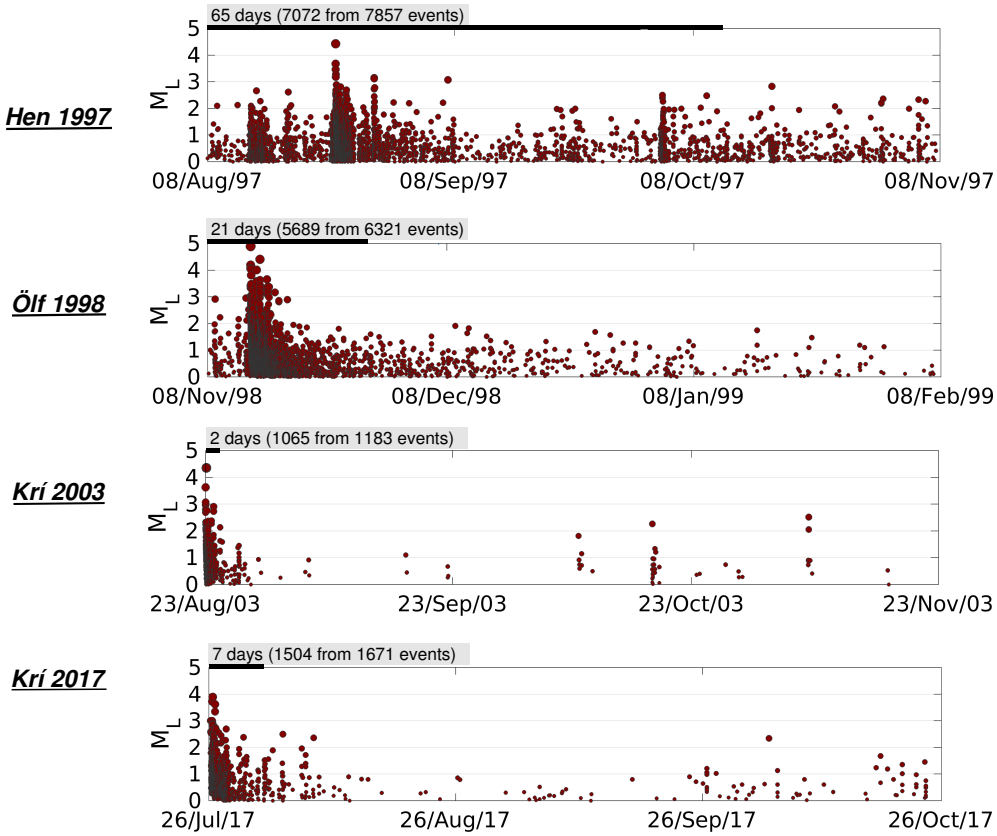

Figure 4.2: Magnitude-time course of the West Bohemian swarms and the 2014 activity (a), and the Southwest Icelandic swarms (b) within 3 months. *Numbers on gray rectangles* - number of days during which 90 % of events, which were recorded within three months, occurred. For the 2014 activity the time interval covers only the M_L4.4 aftershocks (two months indicated by the *dashed black lines*). For acronyms Hen, Ölf and Krí refer to the caption of Table 1.2.

(a)

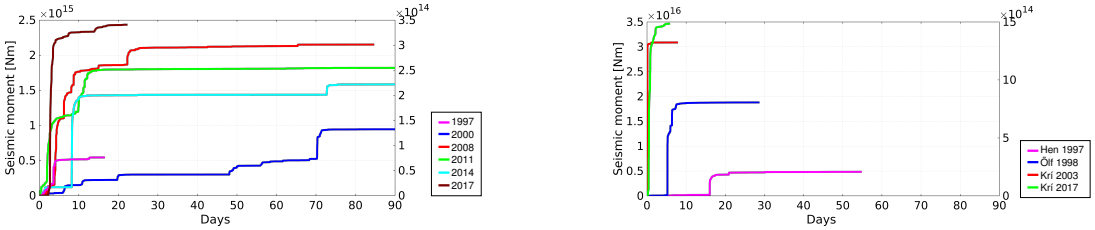

(b)

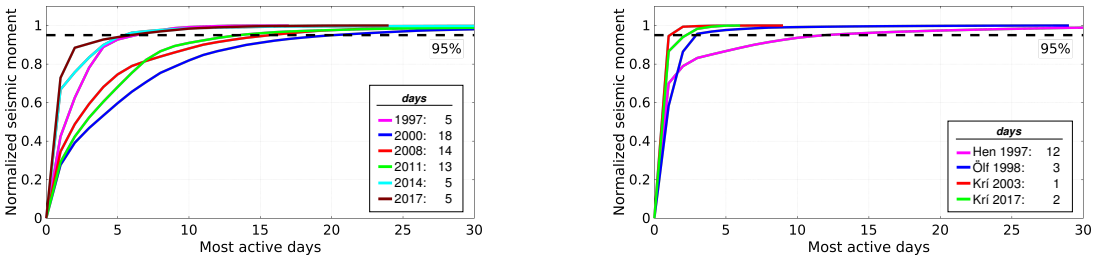

Figure 4.3: (a) Cumulative seismic moment of $M_L \geq 0$ events; (b) normalised cumulative seismic moment by the total seismic moment, sorted based on its daily amount in a descending order. In both (a) and (b): *Left* - West Bohemian swarms, *right* - the Southwest Icelandic swarms. For the colour coding of the individual activities see attached boxes in (a) and (b). *The dashed black line* in (b) - 95% of total seismic moment. *Number of days* in (b) - time necessary to release 95 % of total seismic moment. For the West Bohemian swarms in (a), two vertical axes of the values of seismic moment are shown: the *left axis* is valid for the swarms of 2000, 2008, 2011, and the 2014 activity, the *right axis* is valid for the swarms of 1997 and 2017.

Activity	M_{0tot} [Nm]	M_{Ltot}
1997	7.60×10^{13}	3.5
2000	9.50×10^{14}	4.4
2008	2.15×10^{15}	4.8
2011	1.86×10^{15}	4.7
2014	1.58×10^{15}	4.6
2017	3.41×10^{14}	4.0

Table 4.1: Total seismic moments of the West Bohemia earthquake activities. M_{Ltot} - local magnitude of a hypothetical earthquake corresponding to the given M_{0tot}.

Activity	M_{0tot} [Nm]	M_{Lwtot}
Hen 1997	4.84×10^{15}	5.0
Ölf 1998	1.88×10^{16}	5.4
Krí 2003	3.09×10^{16}	5.5
Krí 2017	1.48×10^{15}	4.7

Table 4.2: The same as in Tab. 4.1 for the Southwest Icelandic swarms. For acronyms Hen, Ölf and Krí refer to the caption of Table 1.2.

4.3 Space-time distribution of events in the West Bohemia and Southwest Iceland earthquake activities

4.3.1 West Bohemian swarm and non-swarm activities and the structure of the Nový Kostel focal zone

The space distribution of the foci of the earthquakes in the main focal zone NK in the period 1994 – 2017 is given in Fig. 4.4. All the activities form a continuous focal belt about 10 km long, striking approximately in the north-south direction. The events are located in depths between 6 and 13 km, however the depth limit for earthquake swarms appears to be 11 km. The focal belt indicates a hidden fault or rather a system of faults. The NK zone comprises a number of fault segments which were separately activated by each West Bohemia activity.

As can be seen from Figs. 4.4 and 4.5, the 2000 and 2008 swarms took place on the same fault segment (segment A), however, they fairly differ in their time course (Fig. 4.2); besides, the 2008 swarm showed much higher seismic-moment rate (Fig. 4.3) and the total seismic-moment released.

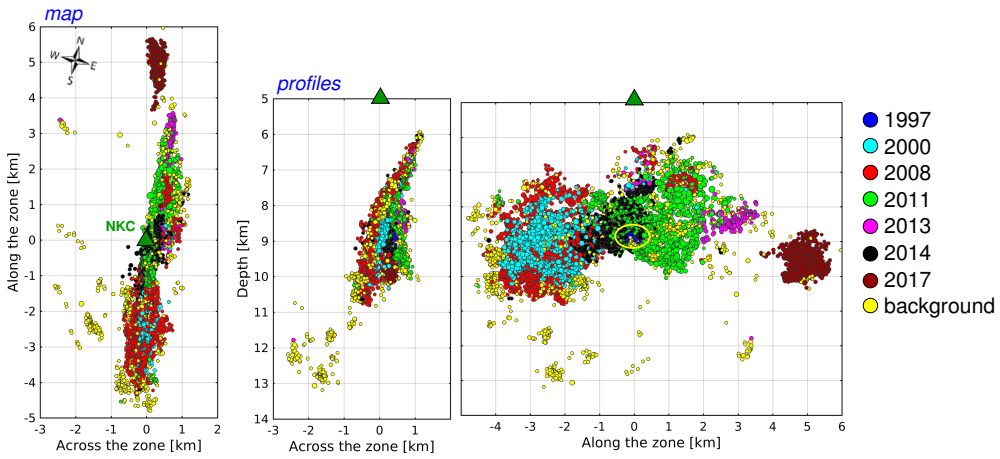

Figure 4.4: Spatial distribution of the earthquake swarms in the period 1997 – 2017 and the non-swarm activity in 2014 in the NK zone. The individual activities are indicated by the colour coding given on the right. *Yellow dots* indicate background activity in the time period of 1994–2017. *Yellow ellipse* highlights the 1997 swarm. The projection is represented by the map view *(left)* and two depth sections, across *(middle)* and along the focal belt *(right)*. The horizontal coordinates are rotated 15° clockwise from the north, the origin corresponds to the location of the central WEBNET station NKC *(green triangle)*.

Event locations of the 2011 swarm disclosed two separately dipping fault segments of a corner-like shape in the northern part of the NK (segments B and C; see Fig. 4.5). The 2013 mini-swarm occurred on segments B and C, thus it appears as a complement of the swarm of 2011. The seismic moment rate in the 2011 swarm is similar to that in the 2008 swarm (Fig. 4.3), the total seismic moment released is a bit lower when compared to M_{0tot} of the 2008 swarm. More details about the 2011 swarm and geometry of segments B and C are given in Čermáková and Horálek (2015).

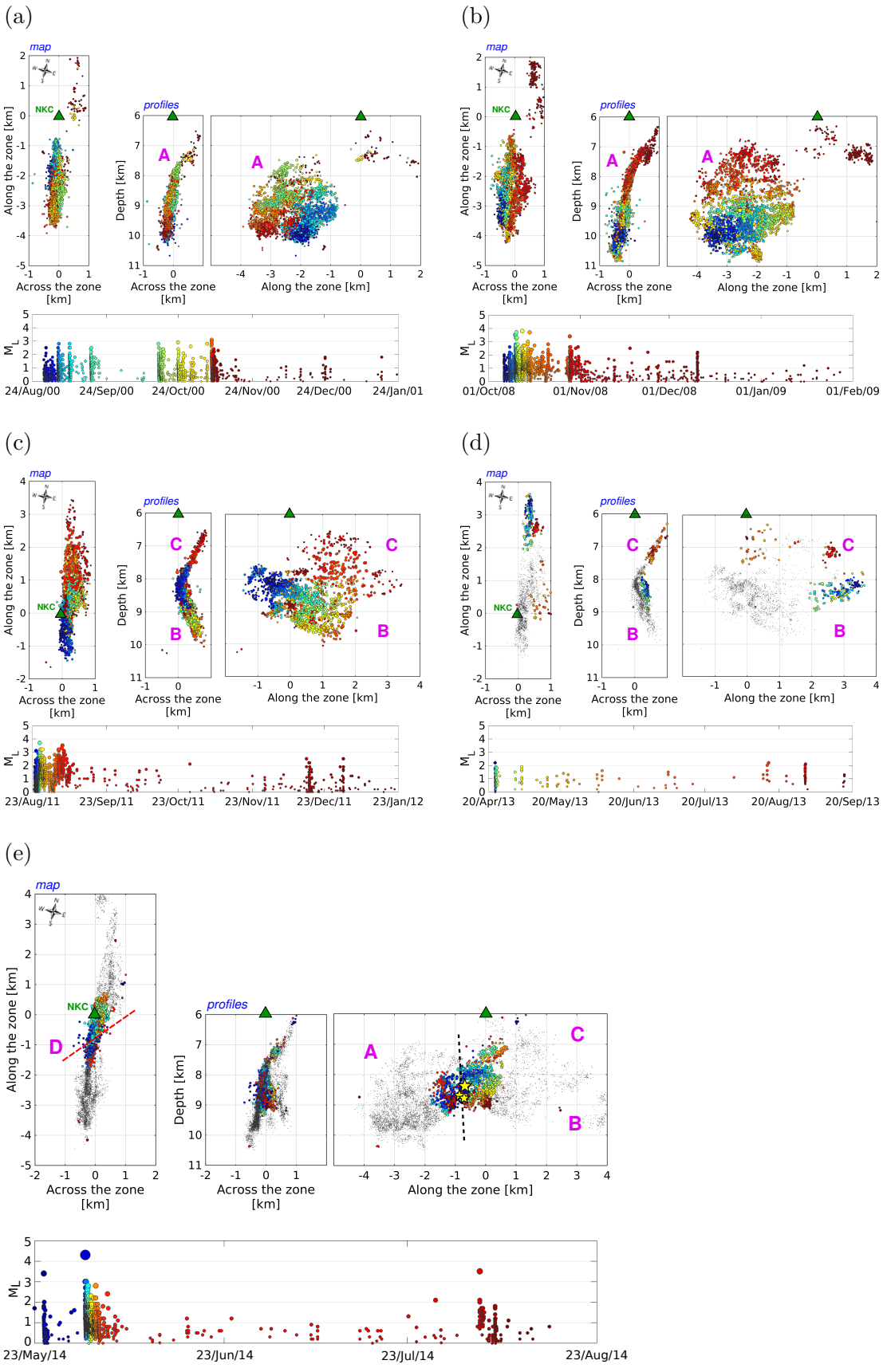
(a)
map
profiles
NKC
A
Along the zone [km]
Across the zone [km]
Depth [km]
M_L
24/Aug/00
24/Sep/00
24/Oct/00
24/Nov/00
24/Dec/00
24/Jan/01
(b)
01/Oct/08
01/Nov/08
01/Dec/08
01/Jan/09
01/Feb/09
(c)
B
C
23/Aug/11
23/Sep/11
23/Oct/11
23/Nov/11
23/Dec/11
23/Jan/12
(d)
20/Apr/13
20/May/13
20/Jun/13
20/Jul/13
20/Aug/13
20/Sep/13
(e)
D
23/May/14
23/Jun/14
23/Jul/14
23/Aug/14

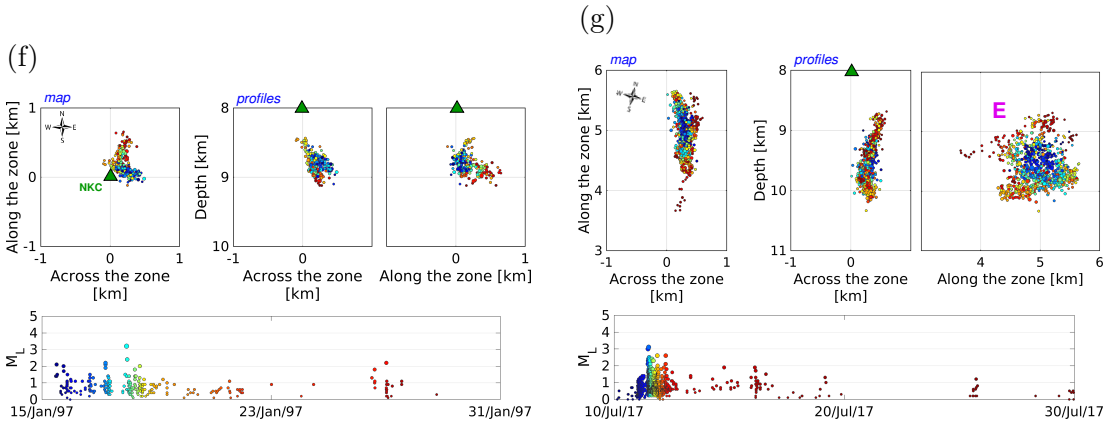

Figure 4.5: Spatio-temporal distribution of events in the West Bohemian swarms of 2000 (a), 2008 (b), 2011 (c), 2013 (d), the 2014 sequence (e), and the swarms of 1997 (f) and 2017 (g). Colour coding in each activity corresponds to the tempotal distribution of events. *Top* in (a) – (g): Distribution of the hypocenters; for the projection and the origin of the horizontal axes refer to the caption of Fig. 4.4. A, B, C, D and E denote fault segments which are bounded by hypocenter clusters. The *yellow stars* in (e) - locations of the three 2014 mainshocks, the *black dashed line* in (e) - the boundary between the southern and northern part of the NK zone. The horizontal coordinates in (a), (b), (e) and (g) are rotated by 15° and in (c) and (d) by 9° clockwise (i.e. by the strike angle of the focal belt). *Pale-gray dots* in (d) mark the 2011 hypocenters, in (e) the 2000, 2008 and 2011 hypocenters. *Bottom* in (a) – (g): Time course of the activity in the magnitude-time plot.

The 2014 mainshock-aftershock activity revealed a small (in terms of size) but significant fault segment (or fault barrier), termed D, which is situated in the transition zone among fault segments A, B and C (Figs. 4.4 and 4.5). Segment D is mainly defined by the three M_L3.5, 4.4 and 3.6 mainshocks because the majority of aftershocks of all the three mainshocks are scattered in fault segments A, B, and C (Fig. 4.6). Therefore, geometry of segment D was estimated from the focal mechanisms of the mainshocks and proved by calculating an equation of the plane defined by the mainshocks hypocenters.

The mainshocks were located close together, mutual distances among them are $|M_L4.4\ M_L3.5| = 410\,\mathrm{m}$, $|M_L4.4\ M_L3.6| = 240\,\mathrm{m}$, and $|M_L3.5\ M_L3.6| = 240\,\mathrm{m}$. I performed a rough estimate of the rupture area of all the three mainshocks to get an idea of the size of segment D. I used two fully independent formulas: (i) by Madariaga (1976) for a circular source:

$$r = kv_rT_d, \tag{4.2}$$

where r is radius of the source, k is a model dependent constant, v_r is the rupture velocity, and T_d is duration of the pulse of the direct P wave, and (ii) by Michálek and Fischer (2013) based on the source spectra of the West Bohemian events which relates the rupture radius r to seismic moment M_0:

$$r = 0.155M_0^{0.206}. \tag{4.3}$$

The estimated radii are shown in Table 4.3.

Formula	$M_L4.4$	$M_L3.6$	$M_L3.5$
Madariaga (1976)	150 m	120 m	130 m
Michálek and Fischer (2013)	180 m	120 m	115 m

Table 4.3: Estimated radii of the rupture area of the 2014 mainshocks.

Although this approach is rather simplified, the radii of the rupture areas estimated by these two independent formulas agree quite well, and besides, the radii for the three mainshocks are comparable to the distances between the events' hypocenters. It implies that the mainshocks represent in fact three-step rupturing of a barrier (segment D) which was a bridge among fault segments A, B and C (black dashed line in Fig. 4.5e).

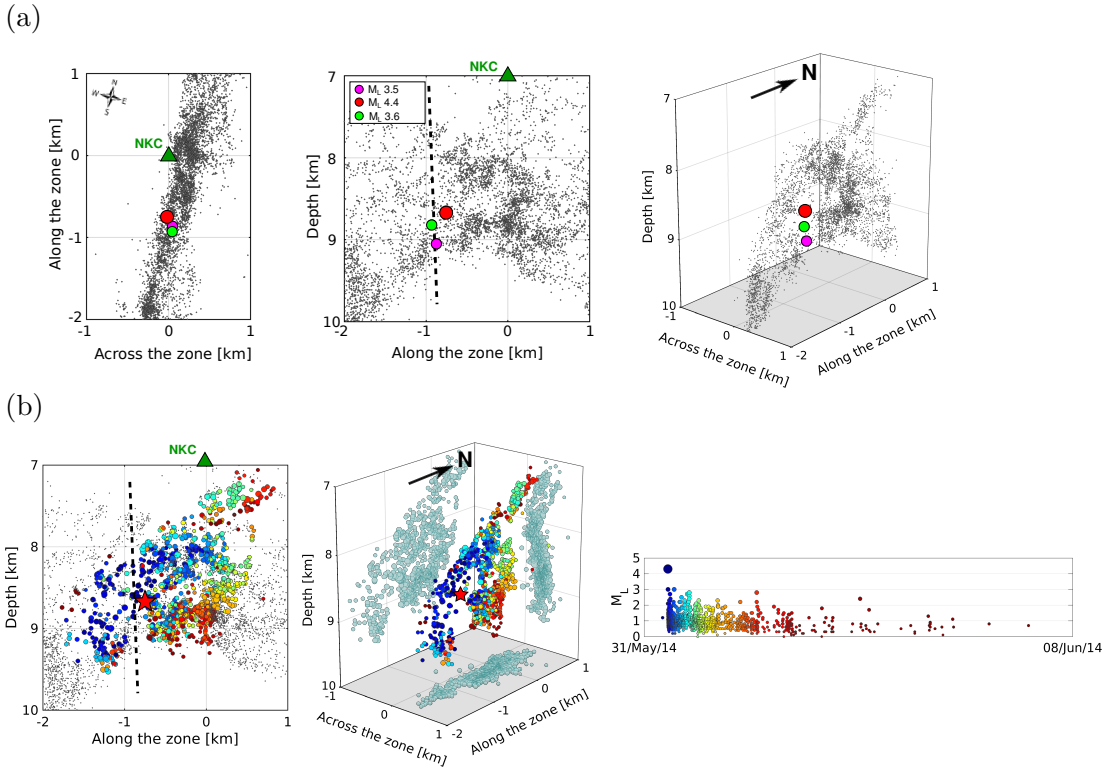

Figure 4.6: (a) Locations of the 2014 mainshocks of $M_L3.5$ (*violet*), $M_L4.4$ (*red*) and $M_L3.6$ (*green*) depicted by the map view (*left*), depth section along the focal zone (*middle*) and 3D view (*right*). (b) Space-time distribution of the $M_L4.4$ mainshock and its aftershocks. The spatial distribution of the foci is represented by the depth section along the focal zone (*left*), and 3D view (*middle*) supplemented by projection onto three perpendicular planes (*light blue dots*). *Grey dots* in the depth section - foci of the 2000, 2008 and 2011 swarms; *black dashed line* - the boundary between the southern and northern part of the NK zone. The temporal distribution of the foci is depicted by the magnitude-time plot (*right*).

The locations of the 2014 aftershocks are the issue. Unlike standard aftershocks that occur randomly along the edges of the mainshock rupture, the 2014 aftershocks occurred not on the mainshock fault D but beyond it along the preexisting oblique fault segments A, B and C. This indicates that the 2014 mainshock-aftershock sequence is rather untypical in relation to common mainshock-aftershock seismicity observed at plate boundary faults. More details about the 2014 non-swarm activity and its comparison with the previous swarms are given in Jakoubková et al. (2017).

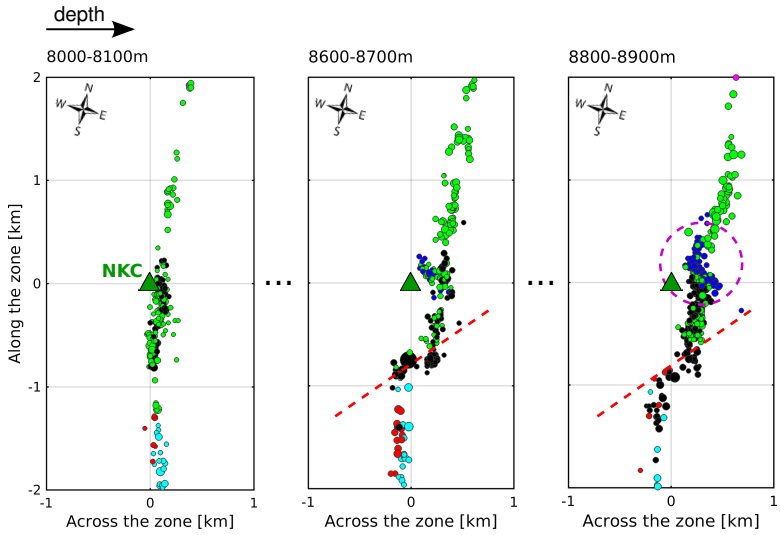

Figure 4.7: Distribution of the foci in the transition area between fault segments A, B and C represented by three horizontal sections at depths of 8000-8100 m (above the 2014 mainshocks), 8600-8700 m and 8800-8900 m (corresponding to depth of the M_L 4.4 and 3.6 mainshocks). The colour-coding matches that in Fig. 4.4. Note a fault jog (middle and right sections) separating the northern segments B and C from the southern segment A being bridged by a fault barrier D (*black dots*). *Red line* - the strike of the barrier indicated by focal mechanisms of the 2014 mainshocks. *Violet dashed circle* highlights a short segment which hosted the 1997 and 2011 swarms, and the 2014 activity.

The 1997 swarm was the first larger West Bohemia/Vogtland earthquake activity after the intense M_L4.6 swarm of 1985/86. It took place in the NK transition area (separating the northern and southern parts of the NK zone) on a corner-like patch (Fig. 4.5) that is located on the edge of segment B (yellow ellipse in Fig. 4.4). A complexity of the transition area is shown in detail in three horizontal sections in depths between 8000 and 8900 m in Figure 4.7. It is evident that the transition area is partitioned into several segments; some of them were repeatedly activated, namely during the swarms of 1997 and 2011 and the 2014 activity (aftershocks). The sections at depths of 8600 – 8700 m and 8800 – 8900 m nicely show that the corner-like patch of the 1997 swarm represents a distinct offset between southern and northern parts of the NK focal zone.

The recent M_L3.1 swarm in July 2017 was specific because of its location and a high rate of the seismic moment release. The swarm events were located in the very north of the NK zone, off the focal belt, indicating a separate segment E (Fig. 4.4).

These analyses allowed me to construct a scheme of the fault structure in the NK zone which is presented in Fig. 4.8. The scheme shows only the major fault segments where the majority of seismic moment has been released. Furthermore, the analyses of the West Bohemian earthquake swarms also point to a gradual northward trend in migration of the swarm activity in the NK zone.

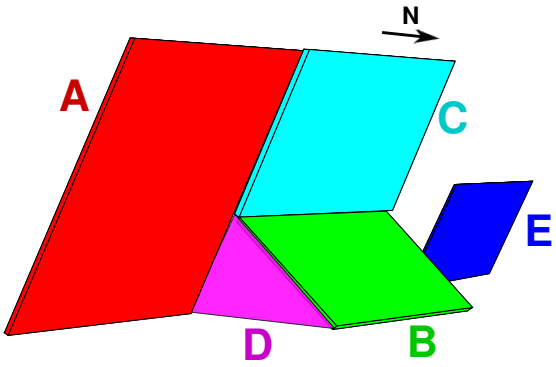

Figure 4.8: Basic scheme of the NK focal zone. Segment A (*red*) was triggered in the 2000 and 2008 swarm, segments B and C (*green and light blue*) in the 2011 swarm, segment/barrier D (*violet*) in the 2014 sequence, and segment E (*blue*) in the 2017 swarm.

4.4 Earthquake swarms in Southwest Iceland from the space-time event distribution point of view

For analysing the space-time distribution of the 1997 Hengill, 1998 Ölfus and 2003 Krísuvík swarms I used data from the SIL catalog. The 2017 Krísuvík swarm events are located in the same way as the West Bohemian ones: the absolute locations applying the NLLoc code to the REYKJANET data and their refinement by the hypoDD code. In order to preserve compatibility I used the SIL velocity model.

The results are given in Figures 4.9 – 4.12. It is obvious that all these swarms are significantly shallower when compared with the West Bohemia ones. The first results indicate the depth limit for the swarm earthquakes is $\sim$6 – 7 km on Reykjanes Peninsula, 8 km in the Hengill volcanic complex, and 10 km in Ölfus area. The patterns of the space-time distribution of the individual earthquake swarms significantly differ but one feature is common: the most of the total seismic moment M_{0tot} in each swarm was released in one short-term phase including a few dominant events (Figs. 4.3a and 4.9 – 4.12).

The swarm in Hengill (M_L4.4) and a subsequent swarm in Ölfus (M_L4.9) are located in close proximity to one another (Fig. 4.13) but their space-time distribution of foci differ substantially. The space-time distribution of the swarm in Hengill (Fig. 4.9) reflects a big complexity of this volcanic complex. The magnitude-time plot indicates several swarm phases, which took place on several different fault segments. The dominant phase corresponds to the N-S striking fault segment (marked 3 in Fig. 4.9).

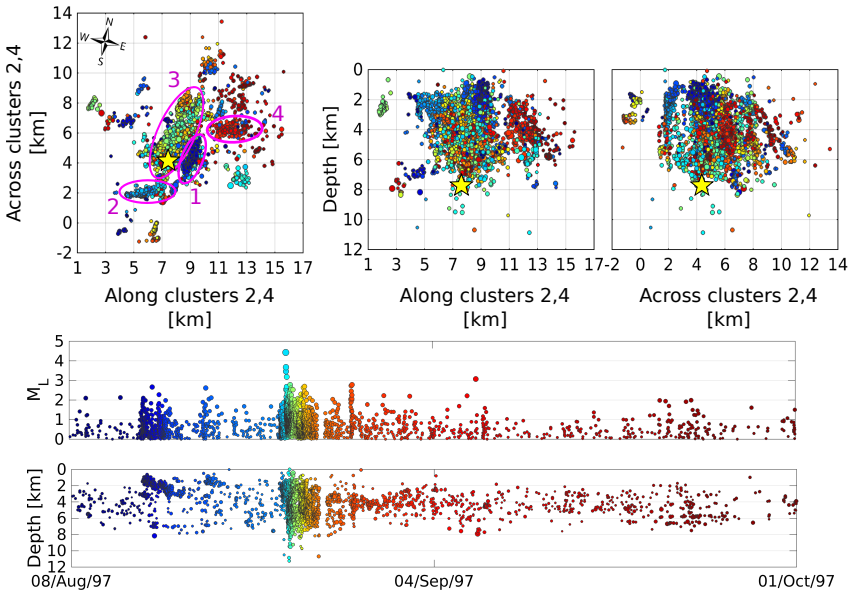

Figure 4.9: Spatio-temporal distribution of events of the Hengill swarm in 1997. Colour coding is proportional to the origin time. *Top* - Distribution of hypocenters (coloured dots) represented by the map view (*left*) and two depth sections, from the south (*middle*) and east (*right*). *Violet numbers* 1 – 4 denote event clusters delineated by *violet ellipses*, which were activated successively during the swarm. The *yellow star* shows location of the strongest event (M_L4.4). The horizontal coordinates are rotated by 13° clockwise (i.e. by an angle that enables distinguishing the event clusters). *Middle* - Time course of the swarm activity in the magnitude-time plot. *Bottom* - Time course of the swarm activity in the depth-time plot.

The M_L4.9 Ölfus swarm was located in the transition area among the eastern Reykjanes Peninsula, Hengill complex and SISZ. It was fairly intense having the total seismic moment released roughly by one order higher than M_{0tot} of the West Bohemia swarms in 2008 and 2011. The focal cluster is quite simple (unlike that of the Hengill swarm) indicating three differently oriented faults/fault segments (marked 1, 2, 3 in Fig. 4.10), all of them have nearly vertical dip. The finding of the intersection of the ENE-WSW and N-S striking faults (1 and 2 in Fig. 4.10) is quite important result. According to Einarsson (2010), the N-S striking faults in the SISZ/Ölfus region are liable for larger strike-slip earthquakes. Interestingly, I found that one of the two mainshocks (M_{Lw}6.3) of the SISZ/Ölfus activity in 2008 was located on the eastern edge of the fault segment 3; moreover, the spatial distribution of the 1998 swarm events corresponds well to the distribution of the 2008 aftershocks (e.g., Brandsdóttir et al., 2010; Li, 2017). It suggests that the N-S striking faults in the area concerned are liable to stronger mainshock-aftershock activities, while the ENE-WSW faults are predisposed to earthquake swarms.

The 2003 a 2017 Krísuvík swarms on the Reykjanes Peninsula were located near each other, at a distance of about 5 km (Fig. 4.14). The 2003 swarm was located in the Krísuvík geothermal field, whereas 2017 swarm beneath the Fagradalsfjall volcano; so, the sites may tectonically differ. The 2003 swarm (M_L4.3) is the most intense activity in terms of the total seismic moment released which I have investigated in my thesis.

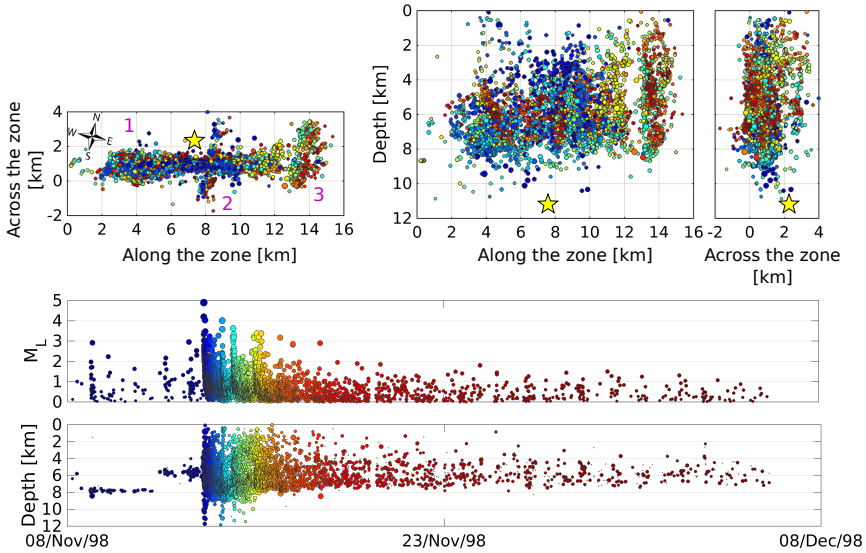

Figure 4.10: Spatio-temporal distribution of events of the Ölfus swarm in 1998. For the figure arrangement, projection and colour coding see Fig. 4.9. Location of the strongest event of M_L4.9 is shown by *yellow star*.

However, both these swarms show a markedly small number of the $M_L \geq 0$ events (event productivity a), particularly that of 2003; for comparison with other Southwest Icelandic and West Bohemian swarms see Tables 1.1 and 1.2. Besides, both swarms exhibit very high rate of the seismic moment release (Fig. 4.3b), which points to the mainshock-aftershock activity.

Prevailing depths of the foci of both 2003 and 2017 swarms (2–5 km) are much smaller than those in the Hengill and Ölfus swarms. The 2003 swarm took place on two differently oriented faults: the primary one striking N-S (marked 1) and the secondary one striking EN-WS (marked 2 in Fig. 4.11). The two faults correspond very well with the tectonic pattern of the Reykjanes Peninsula which is characterized by a series of the N-S oriented faults and NE-SW trending volcanic fissures (Clifton and Kattenhorn, 2006; Einarsson, 2008) (Fig. 4.14).

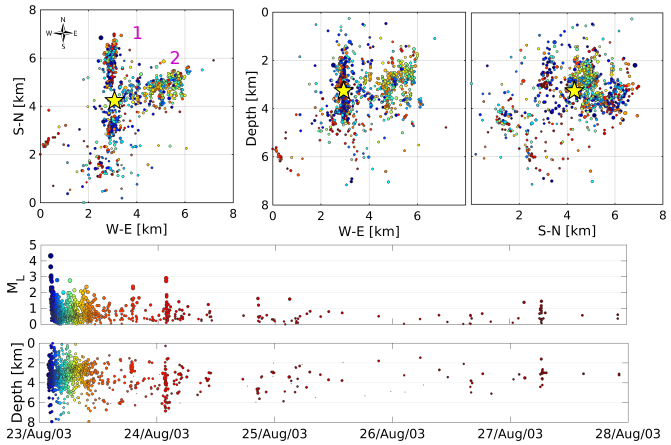

Figure 4.11: Spatio-temporal distribution of events of the Krísuvík swarm in 2003. For the figure arrangement, projection and colour coding see Fig. 4.9; the only difference is that the horizontal coordinates are not rotated. Location of the strongest event of M_L4.3 is shown by *yellow star*.

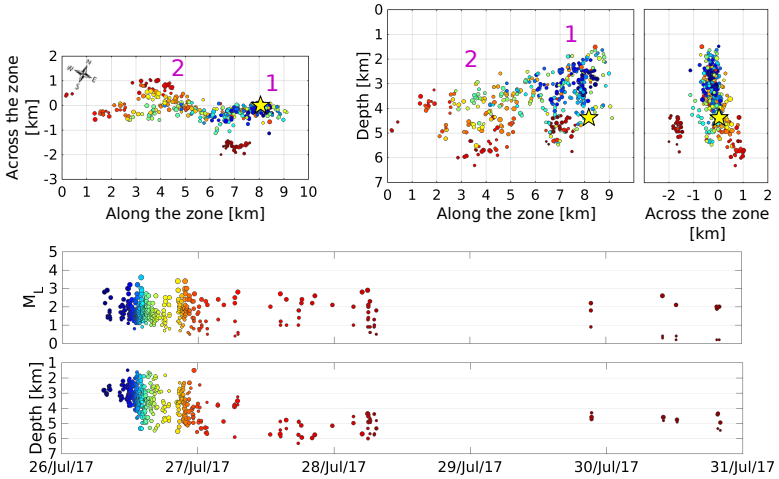

Figure 4.12: Spatio-temporal distribution of events of the Krísuvík swarm in 2017. For the figure arrangement, projection and colour coding see Fig. 4.9; the only difference is that the horizontal coordinates are rotated by 23° clockwise. Location of the strongest event of M_L3.9 is shown by *yellow star*.

The space-time distribution of the 2017 events disclosed two faults, striking ENE-WSW and E-W (1 and 2 in Fig. 4.12) which are parallel or nearly parallel with the MAR plate boundary on the central Reykjanes Peninsula. This is quite important finding because the previous M_L3.0 swarm in 2009 in the Fagradalsfjall area occurred on the N-S fault(s) (Li, 2017). Besides, the E-W and ENE-WSW oriented seismogenic structures on the RP have not been reported in a commonly available literature, yet.

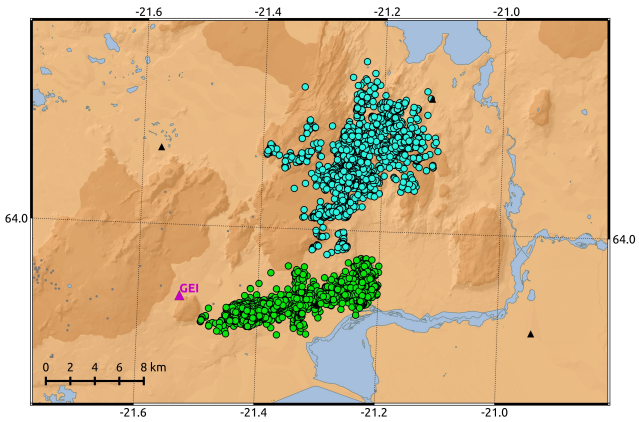

Figure 4.13: Space distribution of swarm events in Hengill in 1997 (*light blue circles*) and in Ölfus in 1998 (*green circles*). *Violet triangles* denote seismic stations of the local REYKJANET network, the smaller *black triangles* represent stations of the regional SIL network.

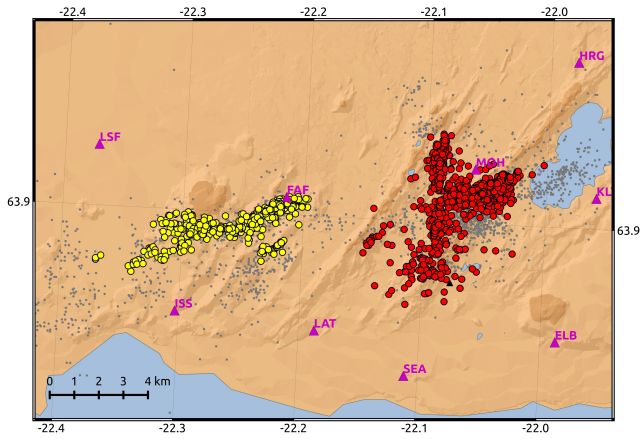

Figure 4.14: Space distribution of swarm events Krísuvík in 2003 (*red circles*) and in 2017 (*yellow circles*). *Violet triangles* denote seismic stations of the local REYKJANET network, the smaller *black triangles* represent stations of the regional SIL network.

4.5 Focal mechanisms in West Bohemia

Focal mechanism is a primary source of information about faulting or rupturing in an earthquake swarm. An important question was whether geometry of the individual faults (fault segments) in the NK zone agrees with prevailing focal mechanisms in the respective activities. As for the mechanisms in the 1997 and 2000 swarms I utilized the moment tensors determined by Horálek et al. (2002) and Horálek and Šílený (2013) and used double-couple (DC) components of resultant MTs.

To estimate the prevailing focal mechanisms in the swarms of 2008, 2011 and 2017 and mechanisms of the 2014 mainshocks, I used the AMT code by Vavryčuk (2011). It inverts P-waves ground displacement amplitudes on the vertical component and provides the full moment tensor. Detailed tests of stability of the 1997 and 2000 source mechanisms are given in Horálek et al. (2002) and Horálek and Šílený (2013). Regarding the 2008, 2011, 2014 and 2017 mechanisms, the stability of the DC components was verified by applying the jack-knife technique to the MT solutions.

Characteristic source mechanisms of the West Bohemian activities are given in Figure 4.15. Two groups of focal mechanisms, the strike-slips with a weak normal (oblique-normal) or thrust (oblique-thrust) component, can be clearly distinguished in each swarm (except the 2017 swarm). The mechanisms of the oblique-normal type prevail in 2000 and 2008 swarms and their predominant strikes and dips fit well geometry of the fault segment A. As regards the 2011 swarm, the oblique-thrust mechanisms are typical for the deeper segment B, while the oblique-normal mechanisms for the shallower segment C. The mechanisms nicely match the segments orientation (for more details refer to Čermáková and Horálek, 2015). Focal mechanisms of the two strongest events in the 2017 swarm are practically identical, of the oblique- normal type fitting well geometry of the segment E.

The source mechanisms of the three 2014 mainshocks are quite similar indicating an oblique-thrust faulting with a significant dip-slip component. Thus they differ significantly from the other swarms, the only similarity was observed in the 1997 swarm (Horálek et al., 2002). The strike, dip, and rake angles for each 2014 mainshock are given in Table 3 in Jakoubková et al. (2017). True fault planes in the 2014 mechanisms were distinguished by calculating an equation of the plane defined by the mainshocks hypocenters. This way we estimated the fault planes striking NE-SW and dipping $\approx 60°$ to SE to be the true fault planes, which suggest geometry of segment D (ruptured barrier).

5. Conclusions

Most of the results in my thesis regarding the West Bohemian earthquake activities have been published in two papers by Čermáková and Horálek (2015) and Jakoubková et al. (2017). The results concerning Southwest Icelandic swarms have been quite fresh, so far unpublished. The results of common analyses can be summarised as follows:

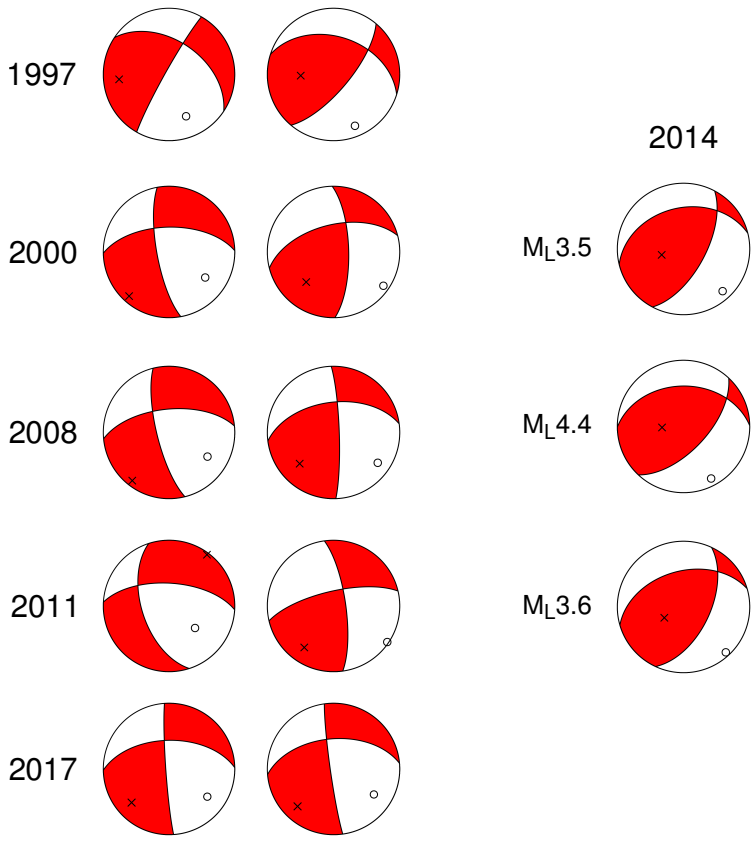

Figure 4.15: Characteristic source mechanisms of the West Bohemian swarms of 1997, 2000, 2008, 2011 and 2017 (*left*), and the three mainshocks of the 2014 activity (*right*). All the fault plane solutions are represented in the equal-area, lower-hemisphere projection. The principal axes P are marked by *circles*, axes T by *crosses*.

(i) Generally, the investigated Southwest Icelandic activities are much larger in terms of magnitudes of the strongest events, total seismic moment released, and in size of the activated focal areas when compared to the West Bohemia ones.

(ii) The West Bohemian and Southwest Icelandic activities show similar magnitude-frequency distribution (b-value ≤ 1.0) and also the interevent time distributions. It implies similar ratio of small to large events and similar event rate in all the activities. The analyses of the GR law also suggest that the swarms comprise overlapping aftershock sequences, each of them dominated by a "mainshock".

(iii) Although the total seismic moment M_{0tot} released in the 2008, 2011 and 2014 West Bohemian earthquake activities is comparable, the parameter a of the GR law (number of the $M_L \geq 0$ events) of the 2014 mainshock-aftershock sequence is significantly lower than that of the 2008 and 2011 swarms. Notably small a value I found for both 2003 and 2017 swarms on the Reykjanes Peninsula, and also for the 1997 swarm in West Bohemia.

(iv) The Southwest Icelandic swarms exhibit much higher rate of the seismic moment release than the West Bohemian ones (although the event rate of both is similar). The West Bohemia swarms are characterised by step by step seismic moment release, whereas one dominant short-term phase is typical of the Southwest Icelandic swarms.

(v) The West Bohemia swarm-like events occur in depths between 6 and 11 km, whereas the Southwest Icelandic swarms are significantly shallower (the smallest depths $\approx 1-2$ km). Our first results indicate the depth limit for swarm earthquakes $\approx 6-7$ km on Reykjanes Peninsula, 8 km in the Hengill volcanic complex, and 10 km in Ölfus area.

(vi) The NK zone comprises a number of fault segments which were separately activated by each West Bohemia activity. The 2000 and 2008 swarms took place on the same fault segment (segment A in our notation), whereas the 2011 swarm disclosed two corner-like oriented fault segments B and C. The three mainshocks in 2014 represent three-step rupturing of the barrier (segment D) in the transition area among segments A, B and C. The 1997 swarm took place on two corner-like patches, one of them embodied in the segment B. A moderate 2017 swarm was located in the very north of the NK zone on a separate fault segment (segment E). The space-time distribution of the NK seismicity suggests a gradual northward trend in migration of the swarm activity in the NK zone.

Prevailing mechanisms in each activity correspond well to geometry of the respective fault segments. Based on that I constructed a scheme of the fault structure in the main focal zone NK that ought to be gradually improved.

(vii) The Ölfus swarm in 1998 represents a continuation of the Hengill activity in 1997, but patterns of their spatial distribution fairly differ. The Hengill pattern indicates a big complexity of this triple-junction volcanic complex comprising number of differently oriented fault segments, while the 1998

Ölfus foci form a single belt which includes one major fault (striking ENE-WSW) crossed by two, nearly perpendicular fault segments (striking N-S). The major fault seems to be predisposed to earthquake swarms whereas the N-S striking faults typically produce single strike-slip earthquakes (Einarsson, 2010). So it is quite probable that the dominant $M_L 4.9$ earthquake of the Ölfus swarm, which was located under the main focal cluster, was a mainshock on a hidden N-S fault which triggered swarm-like seismicity on the ENE-WSW striking faults.

(viii) The 2003 and 2017 swarms on the Reykjanes Peninsula exhibit a strikingly small number of the $M_L \geq 0$ events relative to the other investigated swarms in both West Bohemia and Southwest Iceland. In this respect both swarms resemble the mainshock-aftershock activity. The swarms were located in the rift zone of MAR about 5 km away from each other but their spatial distributions of the foci show different patterns. The 2003 pattern indicates two intersecting faults trending N-S and NE-SW which agrees with tectonics of the RP (e.g., Einarsson, 2010), whereas the pattern of the 2017 swarm shows seismogenic faults parallel or nearly parallel with the MAR plate boundary. This finding is significant because seismogenic structures parallel with the MAR on the Reykjanes Peninsula have not been ordinary reported in geophysical papers dealing with the problems concerned.

(ix) Based on the results of the analyses performed I came to conclusion that most of the West Bohemia earthquake swarms and also the Hengill swarm were series of subswarms with one or more embedded mainshock-aftershock sequences, while both earthquake activities on the Reykjanes Peninsula represent a transition between earthquake swarm and mainshock-aftershock sequence.

Bibliography

R. M. Allen, G. Nolet, W. J. Morgan, K. Vogfjörd, B.H. Bergsson, P. Erlendsson, G.R. Foulger, S. S. Jakobsdóttir, B.R. Julian, M. Pritchard, S. Ragnarsson, and R. Stefánsson. The thin hot plume beneath Iceland. *Geophys. J. Int.*, 137: 51–63, 1999. doi: 10.1046/j.1365-246x.1999.00753.x.

R. M. Allen, G. Nolet, W. J. Morgan, K. Vogfjörd, B. H Bergsson, P. Erlendsson, G.R. Foulger, S. S. Jakobsdóttir, B. R. Julian, M. Pritchard, S. Ragnarsson, and R. Stefánsson. Imaging the mantle beneath Iceland using integrated seismological techniques. *J. Geophys. Res.*, 107/B12:2325, 2002a. doi: 10.1029/2001JB000595.

R. M. Allen, G. Nolet, W. J. Morgan, K. Vogfjörd, M. Nettles, G. Ekström, B.H. Bergsson, P. Erlendsson, G.R. Foulger, S. S. Jakobsdóttir, B.R. Julian, M. Pritchard, S. Ragnarsson, and R. Stefánsson. Plume-driven plumbing and crustal formation in Iceland. *J. Geophys. Res.*, 107/B8:2163, 2002b. doi: 10.1029/2001JB000584.

V. Babuška, J. Plomerová, and T. Fischer. Intraplate seismicity in the western Bohemian Massif (central Europe): A possible correlation with a paleoplate junction. *J. Geodyn.*, 44/3-5:149–159, 2007. doi: 10.1016/j.jog.2007.02.004.

B. Brandsdóttir, M. Parsons, R. S. White, O. Guðmundsson, J. Drew, and B. S. Thorbjarnardóttir. The May 29th 2008 earthquake aftershock sequence within the South Iceland Seismic Zone: Fault locations and source parameters of aftershocks. *Jökull*, 60:23–46, 2010.

H. Čermáková and J. Horálek. The 2011 West Bohemia (Central Europe) earthquake swarm compared with the previous swarms of 2000 and 2008. *J. Seismol.*, 19/4:899–913, 2015. doi: 10.1007/s10950-015-9502-3.

A. E. Clifton and S. A. Kattenhorn. Structural architecture of a highly oblique divergent plate boundary segment. *Tectonophysics*, 419:27–40, 2006. doi: 10.1016/j.tecto.2006.03.016.

P. Einarsson. Plate boundaries, rifts and transforms in Iceland. *Jökull*, 58:35–58, 2008.

P. Einarsson. Mapping of Holocene surface ruptures in the South Iceland Seismic Zone. *Jökull*, 60:117–134, 2010.

T. Fischer, J. Horálek, P. Hrubcová, V. Vavryčuk, K. Bräuer, and H. Kämpf. Intra-continental earthquake swarms in West-Bohemia and Vogtland: A review. *Tectonophysics*, 611:1–27, 2014. doi: 10.1016/j.tecto.2013.11.001.

H. Geirsson, T. Árnadóttir, S. Hreinsdóttir, J. Decriem, P.C. LaFemina, S. Jónsson, R.A. Bennett, S. Metzger, A. Holland, E. Sturkell, T. Villemin, C. Völksen, F. Sigmundsson, P. Einarsson, M.J. Roberts, and H. Sveinbjörnsson. Overview of results from continuous GPS observations in Iceland from 1995 to 2010. *Jökull*, 60:3–22, 2010.

S. Hainzl and T. Fischer. Indications for a successively triggered rupture growth underlying the 2000 earthquake swarm in Vogtland/NW Bohemia. *J. Geophys. Res.*, 107/B12,2338:1–9, 2002. ISSN 0148-0227. doi: 10.1029/2002JB001865.

J. Horálek and J. Šílený. Source mechanisms of the 2000-earthquake swarm in the West Bohemia/Vogtland region (Central Europe). *Geophys. J. Int.*, 194/2: 979–999, 2013. doi: 10.1093/gji/ggt138.

J. Horálek, T. Fischer, A. Boušková, and P. Jedlička. The Western Bohemia/Vogtland region in the light of the WEBNET network. *Stud. Geophys. Geod.*, 44/2:107–125, 2000. doi: 10.1023/A:1022198406514.

J. Horálek, J. Šílený, and T. Fischer. Moment tensors of the January 1997 earthquake swarm in NW Bohemia (Czech Republic): double-couple vs. non-double-couple events. *Tectonophysics*, 356:65–85, 2002.

S. S. Jakobsdóttir. Seismicity in Iceland: 1994-2007. *Jökull*, 58:75–100, 2008.

H. Jakoubková, J. Horálek, and T. Fischer. 2014 mainshock-aftershock activity versus earthquake swarms in West Bohemia, Czech Republic. *Pure and Applied Geophysics*, 175/1:109–131, 2017. doi: 10.1007/s00024-017-1679-7.

M. Khodayar and S. Björnsson. Fault ruptures and geothermal effects of the second earthquake, 29 May 2008, South Iceland Seismic Zone. *Geothermics*, 50:44–65, 2014. doi: 10.1016/j.geothermics.2013.07.002.

T. Lay and T.C. Wallace. *Modern global seismology.* Academic Press, III. series, 1995.

K. L. Li. Location and Relocation of Seismic Sources. Master's thesis, Digital Comprehensive Summaries of Uppsala Dissertations from the Faculty of Science and Technology 1532. 73 pp. Uppsala: Acta Universitatis Upsaliensis. ISBN 978-91-513-0013-9, 2017.

A. Lomax, J. Virieux, P. Volant, and C. Berge. Probabilistic earthquake location in 3D and layered models: Introduction of a Metropolis-Gibbs method and comparison with linear locations. *Advances in Seismic Event Location, Thurber, CH and Rabinowitz, N (eds.), Kluwer, Amsterdam*, pages 101–134, 2000.

A. Lomax, A. Michelini, and A. Curtis. Earthquake location, direct, global-search methods. *Encycl. Complex. Syst. Sci., Part 5, Meyers, RA (ed.), Springer, New York*, pages 2449–2473, 2009. doi: 10.1007/978-0-387-30440-3.

R. Madariaga. Dynamics of an expanding circular fault. *Bull. Seismol. Soc. Am.*, 66/3:639–666, 1976.

J. Málek, J. Horálek, and J. Janský. One-dimensional qP-Wave Velocity Model of the Upper Crust for the West Bohemia/Vogtland Earthquake Swarm Region. *Stud. Geophys. Geod.*, 49/4:501–524, 2005. doi: 10.1007/s11200-005-0024-2.

J. Michálek and T. Fischer. Source parameters of the swarm earthquakes in West Bohemia/Vogtland. *Geophysical Journal International*, 195(2):1196–1210, August 2013. ISSN 0956-540X. doi: 10.1093/gji/ggt286. URL `http://gji.oxfordjournals.org/cgi/doi/10.1093/gji/ggt286`.

K. Mogi. Some discussions on aftershocks, foreshocks and earthquake swarms: the fracture of a semi-infinite body caused by an inner stress origin and its relation to the earthquake phenomena (third paper). *Bull. Earthq. Res. Inst. Univ. Tokyo*, 41:615–658, 1963.

K. Sæmundsson and P. Einarsson. Notes on the Tectonics of Reykjanes. *Report No. ÍSOR-2014/003, ÍSOR, Reykjavík*, 2014.

R. Stefánsson, R. Böðvarsson, R. Slunga, P. Einarsson, S. S. Jakobsdóttir, H. Bungum, S. Gregersen, J. Havskov, J. Hjelme, and H. Korhonen. Earthquake prediction research in the South Iceland seismic zone and the SIL project. *Bull. Seismol. Soc. Am.*, 83/3:696–716, 1993.

P. R. Stoddard and M. T. Woods. Master event relocation of Gorda Block earthquakes: Implications for deformation. *Geophys. Res. Lett.*, 17/7:961–964, 1990. doi: 10.1029/GL017i007p00961.

T. Utsu, Y. Ogata, and R. S. Matsu'ura. The centenary of the Omori formula for a decay law of aftershock activity. *J. Phys. Earth*, 43:1–33, 1995. doi: 10.4294/jpe1952.43.1.

V. Vavryčuk. Principal earthquakes: Theory and observations from the 2008 West Bohemia swarm. *Earth Planet. Sci. Lett.*, 305/3-4:290–296, 2011. doi: 10.1016/j.epsl.2011.03.002.

F. Waldhauser. A computer program to compute double-difference hypocenter locations. *U.S. Geol. Surv. Open File Rep.*, 01-113:1–25, 2001.

F. Waldhauser and W.L. Ellsworth. A double-difference earthquake location algorithm: Method and application to the northern Hayward fault, California. *Bull. Seismol. Soc. Am.*, 90/6:1353–1368, 2000. doi: 10.1785/0120000006.

S. Wiemer and M. Wyss. Minimum magnitude of completeness in earthquake catalogs: Examples from Alaska, the western United States, and Japan. *Bull. Seismol. Soc. Am.*, 90/4:859–869, 2000. doi: 10.1785/0119990114.

J. Woessner and S. Wiemer. Assessing the Quality of Earthquake Catalogues: Estimating the Magnitude of Completeness and Its Uncertainty. *Bull. Seismol. Soc. Am.*, 95:684–698, 2005. ISSN 0037-1106. doi: 10.1785/0120040007.

List of author's publications and citation report

- H. Čermáková and J. Horálek. The 2011 West Bohemia (Central Europe) earthquake swarm compared with the previous swarms of 2000 and 2008. *J. Seismol.*, 19/4:899–913, 2015. doi: 10.1007/s10950-015-9502-3.

  – 7 citations (till August 27, 2018)

- H. Jakoubková, J. Horálek, and T. Fischer. 2014 mainshock-aftershock activity versus earthquake swarms in West Bohemia, Czech Republic. *Pure and Applied Geophysics*, 175/1:109–131, 2017. doi: 10.1007/s00024-017-1679-7.

  – Without citation (till August 27, 2018)